11TH INTERNATIONAL MECHANICAL POWER ENGINEERING
CONFERENCE(IMPEC11),CAIRO, FEB(5-7), 2000

HEAT TRANSFER AND FLUID FLOW CHARACTERISTICS OF FORCED CONVECTION THROUGH A PACKED PIPE

R. A. Khalil, K.M. El-Shazly, and G. R. Assasa [1]
Mechanical Engineering Department,
Zagazig University, Faculty of Engineering-Shoubra,
108 -Shoubra Street, Cairo, Egypt

Abstract

This paper presents a numerical investigation of forced convection heat transfer through a packed pipe that is heated at the surface under constant heat flux. Numerical Computational for steady axisymmetric flow is developed to determine the fluid flow and forced convection heat transfer characteristics through the packed pipe. The formulation of the physical problem is presented by considering the variable porosity and inertia and viscous forces in Darcy model. Heat transfer and fluid flow results are obtained for a wide range of the governing dimensionless parameters. Those, and their respective ranges are Reynolds number based on particle diameter($50 \le Re_d \le 1674$), pipe to particle diameter ratios ($2.67 \le D/d \le 12$) and Prandtl number($0.7 \le Pr \le 5.3$). The finite difference approximation is performed on the basic steady-state governing conservation equations (mass, momentum and energy equations). The momentum equation is expressed numerically using explicit finite difference approximations that is solved using Guass-Seidel method. The energy equation is expressed using implicit finite difference approximations that is solved using Thomas algorithm. The temperature and velocity fields are presented. A correlation between the dependent variable (Nusselt number) and the independent Variables (particle Reynolds number, pipe to particle diameter ratios and Prandtl number) is established. The results show that the average Nusselt number increases with the increase of both particle Reynolds number and Prandtl number. The results of this study show that packing pipes with a porous medium can provide heat transfer enhancement for the same pumping power. The ratio of the average Nusselt number for packed pipe to that of unpacked pipes is nearly two at D/d equals to 2.67 for turbulent flow. This ratio decreases with increasing the ratio of the pipe to particle diameter.

Key Words: Heat transfer- Forced convection-Packed pipe- Porous media

NOMENCLATURE

Symbols

C	specific heat	J/ kg. K
d	particle diameter	m
D	pipe diameter	m

[1]Faculty of Engineering, Mech. Eng. Dept., Shoubra, Zagazig University, Cairo, Egypt.

h	local heat transfer coefficient	W/m^2K
k	thermal conductivity	W / m K
K	permeability	m^2
L	pipe length	m
P	pressure drop	Pa
q	heat flux	W/m^2
r	radial distance	m
R	pipe radius	m
T	temperature	^oC
v	velocity	m/s
v_o	Velocity calculated based on the total area	m/s
z	axial distance from inlet	m

Dimensionless Parameters

Da	Darcy number, K / D^2
D/d	Pipe to particle diameter ratio
F	inertia coefficients
Nu	Nusselt number based on particle diameter, hd / k_f
Pr	Prandtl number, ν / α
p^*	dimensionless pressure drop, $p / (\rho v_o^2)$
Re_d	particle Reynolds number, $v_o d / \nu$
Re_D	Reynolds number based on pipe diameter, $v_o D / \nu$
r^*	dimensionless radial distance, r/D
v^*	dimensionless velocity, v / v_o

Subscripts

b	flow bulk
e	effective
f	fluid
in	inlet
m	average value
o	based on the total pipe area
p	under specific pressure
w	wall
z	axial component
Ds	smooth pipe

Superscript

*	dimensionless
---	average

Greek letters

γ	porous media shape parameter, $\sqrt{\frac{D^2\varepsilon}{K}}$	
ρ	density	kg/m^3
ε	porosity	
∞	ambient	
θ	dimensionless temperature, $\rho C_p v_o (T - Tin) / q$	
ν	kinematic viscosity	m^2/s

1. INTRODUCTION

The number of investigations on convective heat transfer through a saturated porous medium have been on rise during the past decade . This is due to the broad range of many engineering applications such as chemical catalytic reactors, compact thermal collector-storage systems, building thermal insulation, solid matrix heat exchangers, petroleum reservoirs geothermal appertains, packed spheres ground water hydrology and the manufacturing of numerous products in chemical industry. Most of the existing studies deal primarily with the mathematical simplification for porous media based on Darcy law which neglects the effect of solid boundary and viscous and inertia forces. The boundary and inertia effects on forced convective heat transfer in porous media over flat plate were analyzed for a constant porosity of a porous medium by Vafai and Tien,1980. These effects were shown to play a significant role in highly permeable media, high Prandtl number fluids and large pressure gradients. The measurements of Benenati and Brosilow, 1962, show a distinct porosity variation in packed beds. Their results show a high porosity region close to the external boundary. The porosity as a function of the distance from the boundary can be obtained from these measurements.

Some investigators[7,17] indicated that the variable porosity close to an impermeable boundary leads to a number of important effects such as flow mal-distribution and channeling due to the presence of the maximum velocity in a region near the external boundary. They used these measurements to solve numerically the velocity profile for air through packed beds. However, their results were limited because the general formula of the momentum equation was not applied. Vafai, 1984, studied theoretically the effect of flow channeling on forced convection over flat plate while Poulikakos & Renken, 1987, investigated this phenomenon theoretically for forced convection in the fully developed thermal entrance length in channel filled with porous medium. Vafai et al, 1985, studied the boundary layer and forced convection for a matrix consisting of 5 and 8 mm diameters packed spheres over flat plate. Comparison of experimental and numerical results were presented for average Nusselt number as a function of Reynolds number based on pore diameter. Numerical results for local Nusselt number and temperature distributions were also presented. A significant difference was found in flow and temperature distributions and heat transfer coefficient when compared with the results of Darcy model.

The present work is a numerical investigation to study heat transfer and fluid flow characteristics of forced convection through a horizontal cylinder filled with a porous medium. A numerical simulation is performed to study the effect of Reynolds number, fluid properties and porous media on both fluid flow and heat transfer characteristics. A correlation between the dependent variable (average Nusselt number) and the independent variables (particle Reynolds number, Prandtl number and pipe to particle diameters ratio) has also been obtained.

2 PROBLEM FORMULATION

2.1 Governing Equations

Steady state axisymmetric flow through a packed pipe as shown in Fig.1 is considered. The porous medium is considered to be homogenous, isotropic and saturated with a fluid. Also, the fluid is assumed to be in local thermal equilibrium with the solid matrix. The pipe surface is heated under constant heat flux and the fluid has a constant inlet temperature. Momentum and energy equations are derived based on the local average technique where the effects of variable porosity, inertia and viscous forces are considered. The governing equations are expressed with the above assumptions in dimensionless form as disccused in Khalil, 1999, as;

1-Continuity equation

$$\frac{\partial v_z^*}{\partial z^*} = 0 \tag{1}$$

2-Momentum equation

$$0 = -\frac{\partial p^*}{\partial z^*} + \frac{1}{\varepsilon \, Re_D} \frac{1}{r^*} \frac{\partial}{\partial r^*}\left(r^* \frac{\partial v^*_z}{\partial r^*}\right) - \frac{1}{Re_D \, Da} v_z^* - F\varepsilon^{0.5} \gamma v_z^{*2} \tag{2}$$

3-Energy equation

$$v_z^* \frac{\partial \theta}{\partial z^*} = \frac{1}{\varepsilon \, Re_D \, Pr} \frac{\partial^2 \theta}{\partial z^2} + \frac{1}{\varepsilon \, Re_D \, Pr} \frac{1}{r^*} \frac{\partial}{\partial r^*}\left(r^* \frac{\partial \theta}{\partial r^*}\right) \tag{3}$$

2-2 Non-Dimensional Boundary Conditions

The boundary condition equations may be given in a dimensionless form as;

1- at inlet

$$\theta(0, r^*) = 0 \tag{4}$$

2-at the wall

$$v^*(z^*, 0.5) = 0; \tag{5}$$

$$\frac{\partial \theta}{\partial r^*} = \frac{\rho C_p v_o Dq}{k_e} \tag{6}$$

3- at the exit

$$\frac{\partial \theta}{\partial z^*} = 0 \tag{7}$$

4- on the center line

$$\frac{\partial \theta}{\partial r^*} = 0 \tag{8}$$

$$\frac{\partial v^*}{\partial r^*} = 0 \tag{9}$$

Also, momentum and energy equations are written according to L'Hospital rule as explained in Sayed, 1992;

$$0 = -\frac{\partial p^*}{\partial z^*} + 2\frac{1}{\varepsilon \, Re_D} \frac{\partial}{\partial r^*}\left(\frac{\partial v^*_z}{\partial r^*}\right) - \frac{1}{Re_D \, Da} v_z^* - F\varepsilon^{0.5} \gamma v_z^{*2} \tag{10}$$

$$v_z^* \frac{\partial \theta}{\partial z^*} = \frac{1}{\varepsilon \, Re_D \, Pr} [\frac{\partial^2 \theta}{\partial z^2} + 2 \frac{\partial}{\partial r^*} (^* \frac{\partial \theta}{\partial r^*})] \quad (11)$$

2-3 Local and Average Nusselt Number

Local convective heat transfer coefficient can be calculated at any section from,

$$h = \frac{q}{(T_w - T_b)};$$

Local convective heat transfer coefficient may be integrated to get the average convective heat transfer coefficient as

$$\bar{h} = \frac{1}{L} \int h dz$$

where, L is length of the pipe.

Then local and average Nusselt numbers are calculated from $Nu = \frac{hd}{k_f}$ and $\overline{Nu} = \frac{\bar{h}d}{k_f}$ respectively

3. NUMERICAL PROCEDURE

Finite difference method is known to be successful in solving similar partial differential equations as explained in Bejan, 1984, and Steven et al , 1989. To overcome the nonlineartiy of convective term, the second up-wind differencing method explained by Bejan, 1984, is introduced in the present model. The linearity of inertia term is solved using the tangent-linearization method explained in Patanker, 1980.

3.1 Computational Approach

Momentum equation is expressed using explicit finite difference approximations that is solved by Guass-Seidel method. Energy equation is expressed using implicit finite difference approximations and that is solved using Thomas algorithm. In this scheme, the velocity and temperature are given a guessed values at all interior nodes in the beginning of the solution. In obtaining the numerical results, the following input parameters are introduced to the computer programs: the driving pressure gradient, the particle diameter and the thermophysical properties of the fluid and the porous media. The driving pressure force , porosity, and permeability are calculated from Benenati & Brosilow,1962, and Vortmeyer & Schuster, 1983. Equation(2) is solved to get the velocity distributions in the radial direction. After reaching a convergence solution for the momentum equation, the obtained velocity distributions are checked for satisfying the continuity equation. The program begins to calculate the temperature distributions from inlet to exit section where the temperature is known at inlet section and from the heated wall to the center node where the boundary condition of constant heat flux is known. The finite difference equation is written for every node such that each axial step represents a tri-diagonal matrix. This space-saving modification is advantageous because the resulting algorithm requires less computer memory. Thomas algorithm is used to solve the resulting tri-diagonal matrix.

3.2 Numerical Stability and Convergence

To judge the iterative convergence of the solution for the present computations, the following criterion is used

$$\left|\frac{\xi^{k}-\xi^{k-1}}{\xi^{k}}\right| \leq 5x10^{-5}$$

at each point in the domain for both the temperature and velocity. The superscript k represents the present iteration .

In order to properly select the mesh size, many runs are made to select the suitable mesh size which gives better accuracy. It is observed that the use of the dense mesh is advantages and more reasonable for the range of study of particle Reynolds number and pipe to particle diameters ratio owing to the variable change of porosity near the wall which causes significant changes in magnitude of the velocity. Computations are carried out with 10x10 to 100x100 uniform grid. Fig.2 shows the effect of mesh size on the average Nusselt number for (D/d) equal to 2.67 and particle Reynolds number 3008. The present model has good stability and the solution is convergence at a mesh size greater than 30x30.

It is necessary to check the validity of the present numerical results. Therefore, a comparison of the present numerical results with previously published work was carried out. Chi-Hsiung and Finlayson, 1977, presented and listed correlations for the average Nusselt number for air as a fluid flows through the porous medium as:

$$\overline{Nu} = 10.7 + 0.033\,Re_d\,Pr \qquad (12)$$

$$\overline{Nu} = 0.155\,Re_d^{0.75}\,Pr^{0.333} \qquad (13)$$

Good agreement for average Nusselt number between the present numerical results and the above correlations is obtained at Prandtl number of 0.7 as shown in Fig.3. Figure 4 shows a good agreement between the numerical results represented in the average Nusselt number based on the pipe diameter and the numerical results of Hunt and Tien, 1988, at low Reynolds number.

4. RESULTS AND DISCUSSIONS

4.1 Fluid Flow

Many computational runs are performed covering a wide range of the governing parameters for particle Reynolds number up to 3751 and pipe to particle diameters ratio($16 \leq D/d \leq 2.66$) at $0.7 \leq Pr \leq 5.3$ to calculate the velocity distributions.

Many of previous researches such as Fand &Thinakaran, 1990 , Hunt& Tien,1988, and Vortmyer and Schuster,1983, correlated the porosity function based on the experimental measurements of Benenati and Brosilow, 1962. The value of the porosity at the wall is not accurately specified. Many of these researchers considered the porosity equals to unity at the wall. The numerical results for the velocity distributions obtained in the present study are compared with previously published results. This comparison is shown in Fig.5. The analytical solution of Vortmeryer and Schuster, 1983, considered the general model with porosity at the wall is taken as unity. Figure 5 shows that the bypass flow occurs near the wall due to the presence of the high permeability at this region. Also, this figure shows a large deviation between the analytical solution of Vortmeryer and Schuster, 1983,)and the measurements listed in the same reference above the surface of the solid particles at the bed exit. This may be due to considering the porosity at the wall is unity which causes the observed channeling and bypass flow phenomena near the pipe . But Beavers et al., 1973, and the previous studies listed in Vortmeryer and Schuster, 1983, limited the porosity at the wall to a value $0.44 \leq \varepsilon_w \leq 0.56$, so that the porosity at the wall is limited from 0.44 to 0.56 in the present model. Figure.4 shows a good agreement between the present numerical solution

and the measurements listed in Vortmeryer and Schuster, 1983, when the porosity at the wall is considered 0.44. Figure 6 shows the effect of grain size and different flow rates on the velocity profiles . It is observed that the pore velocity increases with increasing the pipe to particle diameter ratios as shown in Fig.6a. This is due to the decrease of the porosity at high pipe to particle diameter ratios. Also, the maximal velocity is closer to the wall at high pipe to particle diameter ratios for the same mass flow rate. This is due to the fact that the layer which has a high permeability has a narrow width at high pipe to particle diameter ratios.

Considering the limitation of the porosity at the wall from 0.44 to 0.56, a nearly uniform porosity distribution is obtained at large grain size in the packed pipe. Examining Fig.6a, it is observed that the channeling phenomena decreases at large grain size. This may be attributed to the nearly uniform porosity distribution at low ratio of pipe to particle diameters .

Figure.6b shows the effect of flow rate on the velocity profiles at (D/d) equal to 3.2. It is obvious that the decrease of flow rate increases the pore velocity. This may be attributed to the decrease of inertia and viscous effects at low flow rate and the increase of the dimensionless pressure gradient.

4.2 Heat Transfer

4.2.1 Temperature Distributions Inside The Porous Medium

Figure.7 presents typical temperature distributions in the radial distance r/R at different axial distances z/D for some selected values of flow rate and pipe to particle diameter ratios respectively .

From Fig.7, it is clear that the presence of the porous medium increases the rate of heat transfer due to the mixing between the fluid layers which increases the turbulence level. This is obviously observed in Fig.7a such that the temperature gradient in radial direction decreases with the increase of flow rates. Figure.7a shows that increasing of the particle Reynolds number due to increasing of the flow rate ($Re_d = 595$) leads to decrease of the temperature difference at z/D equal to 40 and 88 in comparison of ($Re_d = 170$) . This is relative to the total decrease in the temperature difference between the inlet and exit temperatures of the fluid.

Figure.7b shows that the values of temperatures along radial direction for D/d=4 are greater than those for D/d =16 at a certain value of dimensionless axial distance. This is due to the fact that the channeling phenomena increases with decreasing the particle diameter which increase the heat transfer rate and consequently decrease the pipe-surface temperatures.

4.2.2 Surface and Flow Bulk Temperature Distributions in the Axial Direction.

Figure 8 shows pipe surface and flow bulk temperature distributions for typical values of flow rate and pipe to particle diameters ratio. It is clear that the pipe surface and the flow bulk temperatures increase linearly and nearly at the same rate which is similar to the unpacked pipe. Figure 8a shows the effect of the particle Reynolds number due to the increase of the flow rate on the pipe-surface and flow bulk temperature distributions against the axial distance for D/d equal to 6.4. This figure shows that values of pipe surface and flow bulk temperatures along axial direction decrease with increasing particle Reynolds number from 170 to 595 due to the increase of the flow rate .

Figure 8b shows the effect of the particle Reynolds number due to the change of the particle size on the axial pipe surface and flow bulk temperatures inside the porous medium. The particle size has a slight effect on the temperature distributions as shown in Fig.8b. It is

observed that pipe surface and flow bulk temperatures increase when the particle size increases. This may be attributed to the decrease of the pore velocity and channeling effect at large grain size which leads to the decrease of the rate of heat transfer from the pipe surface.

4.2.3 Local and Average Nusselt Number Distributions

The heat transfer rate in terms of local and average Nusselt numbers are computed for a wide range of the governing parameters $170 \le Re_d \le 1674$, $2.66 \le D/d \le 16$ for different Prandtl number ($0.7 \le Pr \le 5.3$)

Figure.9 shows the effect of the particle Reynolds number on the local Nusselt number at the inner surface for $30 \le Re_d \le 1674$ at Prandtl number equal to 5. From this figure, it is clear that the local Nusselt number decreases with the axial distance in the flow direction. Then, it reaches an asymptotic value at the fully developed region of the packed pipe. From Fig.9, it is clear that the increase of particle Reynolds number increases the local Nusselt number. This can be attributed to the fact that the presence of the porous medium increases the rate of heat transfer due to the mixing between the fluid layers. Figure 10 shows the effect of Prandtl number on the average Nusselt number. As the Prandtl number increases, the Nusselt number increases.

5. NUSSELT NUMBER CORRELATION

Many of computational runs are performed covering a wide range of the governing parameters(Particle Reynolds number, pipe to particle diameters ratio and Prandtl number). Generally, the present numerical results for heat transfer in terms of average Nusselt numbers may be correlated as:

$$\overline{Nu} = 3.5 + \frac{0.064465\,Re_d^{0.8886}\,Pr^{0.7725}}{\left(\frac{D/d}{D/d+9.3779}\right)^{0.09967}} \qquad (14)$$

$50 \le Re_d \le 1600$

$0.7 \le Pr \le 5.4$

$2.67 \le D/d \le 12$

The properties of the fluid are calculated at the arithmetic mean temperature of the inlet and the exit of the pipe. The maximum deviation from the computed values is 22% which is occurd at either low particle Reynolds number and small pipe to particle diameter ratios or high particle Reynolds number and large pipe to particle diameter ratios.

6. EVALUTION OF HEAT TRANSFER RATE ENHANCEMENT

An evaluation of heat transfer enhancement achieved by packing a pipe with a porous medium is carried out by comparing the average Nusselt number for the packed pipe with that of unpacked (smooth) pipe (where parameters designated by subscript Ds). The average Nusselt number and friction factor for fully developed turbulent flow in smooth pipe with uniform heat flux at the pipe-surface are given in Holman, 1986.

$$Nu_{Ds} = \frac{(f_{Ds}/8)\,Re_{Ds}\,Pr}{1.07 + 12.7(f_{Ds}/8)^{0.5}(Pr^{2/3}-1)} \qquad (15)$$

where the friction factor

$$f_{Ds} = (1.82 + \log_{10} Re_{Ds} - 1.64)^{-2} \qquad (16)$$

Using Eq.(14&15) and the calculations of the pressure drop of packed and unpacked pipes, the enhancement ratio(ratio of average Nusselt number for a packed pipe to that for an unpacked (smooth) pipe) can be calculated for turbulent flow. Figure.11 shows the enhancement ratio of packed pipe with D/d of 2.67, 3.93 and 7.9 under the constraint of equal pumping power. This figure shows that the enhancement ratio achieved with D/d=3.92 is about 75 % more than for that achieved with D/d=7.9. The results show that decreasing the particle size decreases the enhancement ratio due to the increase of the pressure drop. Finally, the results of this study show that for equal pumping power the method of packing with porous media provides equal to about two times those of unpacked pipes for small pipe to particle diameters ratio(D/d=2.67). However, increasing this ratio decreases the enhancement ratio.

8.CONCLUSIONS

A correlation between the dependent variable (Nusselt number) and the independent Variables (particle Reynolds number, pipe to particle diameter ratios and Prandtl number) is established. Good agreement between the numerical and the previously-published measurements for the velocity distributions through the packed pipe when considering the porosity at the wall from 0.44 to 0.56 was found. The pore and channeling phenomena increases as the particle Reynolds number decreases due to the decrease of the particle size for the same flow rate. For small pipe to particle diameters ratio($D/d \leq 2.0$), the channeling phenomena is not observed for different flow rate. Also, for different Prandtl number, the flow exhibits the same velocity profiles.

The temperature distributions have a low temperature gradient in the radial direction. The local pipe-surface and flow bulk temperatures increase linearly in the axial direction and nearly at the same rate in the thermal fully developed length.

The local Nusselt number reaches its asymptotic value at a distance from the inlet of the heating section equal to (8-10) times the diameter of the pipe. The average Nussult number almost increases with increasing both particle Reynolds and Prandtl numbers. The results of this study show that packing the pipes with a porous medium can provide heat transfer enhancement for the same pumping power.

REFERENCES

1-Benenati, R. F. and Brosilow, C. B. , " Void Fraction Distribution in Beds of Spheres", A. I. Ch. E. Journal, Vol. 8, No. 3, pp. 359-361, 1962.

2-Beavers, G. S., Sparrow, E. M. and Rodenz, D. E. " Influence of bed size on the flow Characteristics and porosity of Randomly packed beds of spheres" Journal of Applied Mechanics, pp 655-660, Septemer, 1973.

3-Bejan, A. "Convective Heat Transfer ", John Wiley & Sons, NewYork 1984.

4-Chi-Hsiung, Li and Finlayson, B. A., " Heat Transfer in Packed Beds- A Reevalution", Chemical Engineering Science, Vol. 32, pp.1055- 1066, 1977.

5-Fand, R. M. and Thinakaran, R. " The Influence of the Wall on Flow Through Pipes Packed With spheres", Transactions of the ASME, Vol. 112, pp84-88, March 1990.

6-Holman, J., "Heat Transfer", MacGraw-Hill , NewYork, 1986

7-Hunt, M. L. and Tien, C. L., " Non Darcian Convection in Cylindrical Packed Beds" Transactions of the ASME, Vol. 110, pp378-384, May 1988.

8-Kahlil, R. A. "Experimental and Numerical Investigation of Forced Convection Heat Transfer In a packed Pipe" M. Sc. Thesis, Zagazig University, Faculty of Engineering , Shoubra, 1999.

9-Patankar, S. V.,"Numerical Heat Transfer and Fluid Flow ", MacGraw-Hill ,NewYork, 1980
10-Poulikakos, D. and Renken, K. "Forced Convection in a Channel Filled With Porous Medium, Including the Effects of Flow Inertia, Variable Porosity, and Brinkman Friction ", Transaction of the ASME Vol. 109, pp. 880-888, November 1987.
11-Steven, C. Charra, and Raymond, P. Canale " Numerical Methods for Engineering", MacGraw-Hill , NewYork, 1989.
12-Sayed, A. A. " Heat Transfer to Air-solids Turbulent Flow in Pipes ", Ph. D. Thesis, Faculty of Engineering, Cairo university, 1992
13-Vafai, K. and Tien, C. L., "Boundary and Inertia Effects on Flow and Heat Transfer in Porous Media", Int. J. Heat Mass Transfer, Vol. 24, No. 3, pp. 195-203, 1980.
14-Vortmeyer, D. and Schuster, J. , "Evalution of Steady Flow Profiles in Rectangular and Circular Packed Beds by a Variational Method ", Chemical Engineering Science Vol. 38, No. 10, pp. 1691-1699, 1983.
15-Vafai, K., " Convective Flow and Heat Transfer in a Variable-Porosity Media ", J. Fluid Mech., Vol. 147, pp. 233-259, 1984.
16-Vafai, K., Alkire, R.L. and Tien, C. L. "An Experimental Investigation of Heat Transfer in Variable Porous Media", Transactions of the ASME, Vol. 107, August 1985, pp.642-647.
17-White, S. M. and Tien, C. L. , " Analysis of Flow Channeling Near the Wall in Packed Beds ", Warme-und Stoffubertragung 21, 291-296, 1987

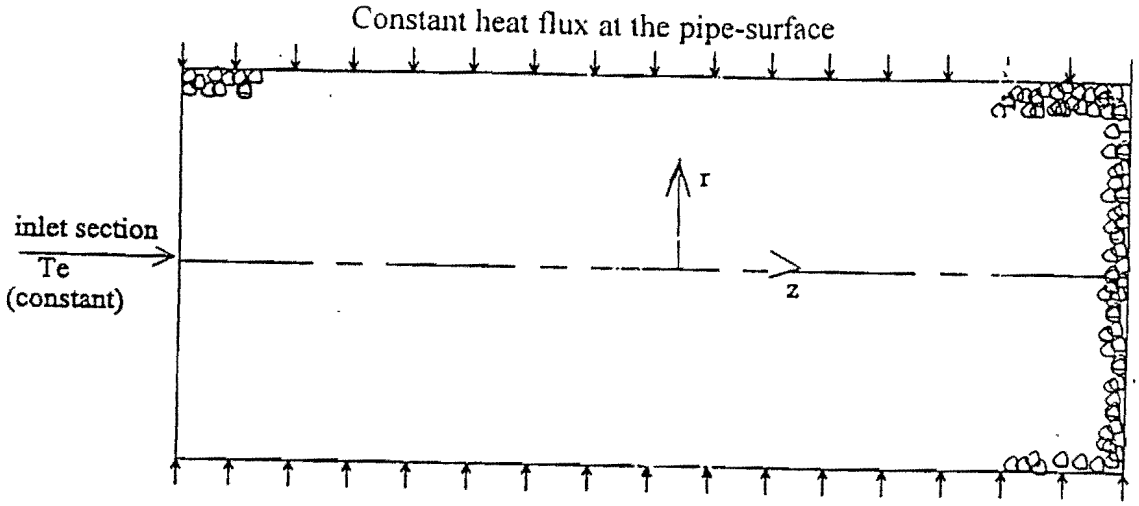

Fig. 1 Physical model of the horizontal pipe, coordinate system and the boundary conditions

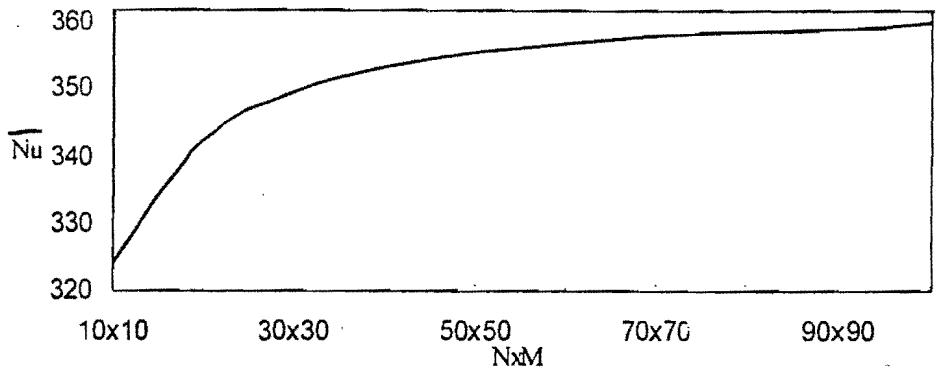

Fig.2 Effect of mesh size on the average Nusselt number based on the particle diameter(Re_d=3008.5, Pr=5.16 and D/d=2.67)

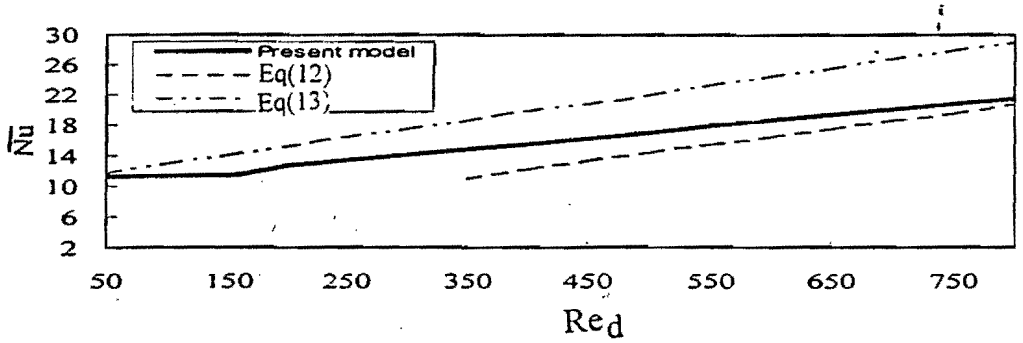

Fig.3 Comparison of the average Nusselt number between the present numerical and previously published results(average Nusselt number based on particle diameter) (D/d=4.78, Da=4.3x10-5 γ =96.12 and Pr=0.7)

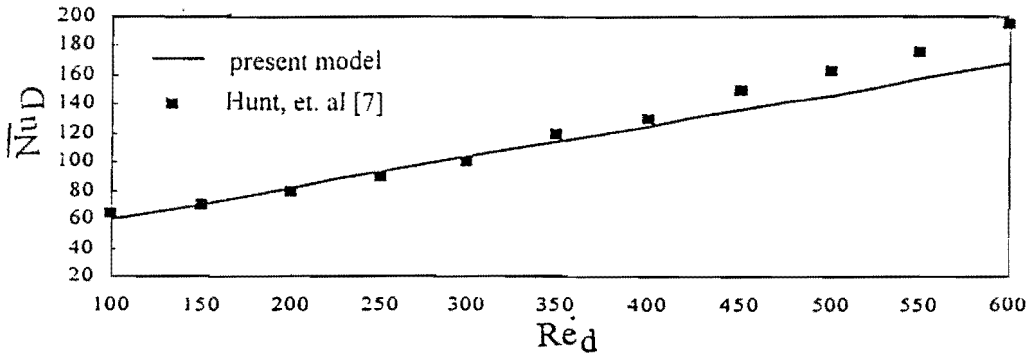

Fig.4. Comparison of the average Nusselt number between the present numerical and previously published results(average Nusselt number based on the pipe daimeter) (D/d=4.78, Da=4.3x10^{-5} γ =96.12 and Pr=0.7)

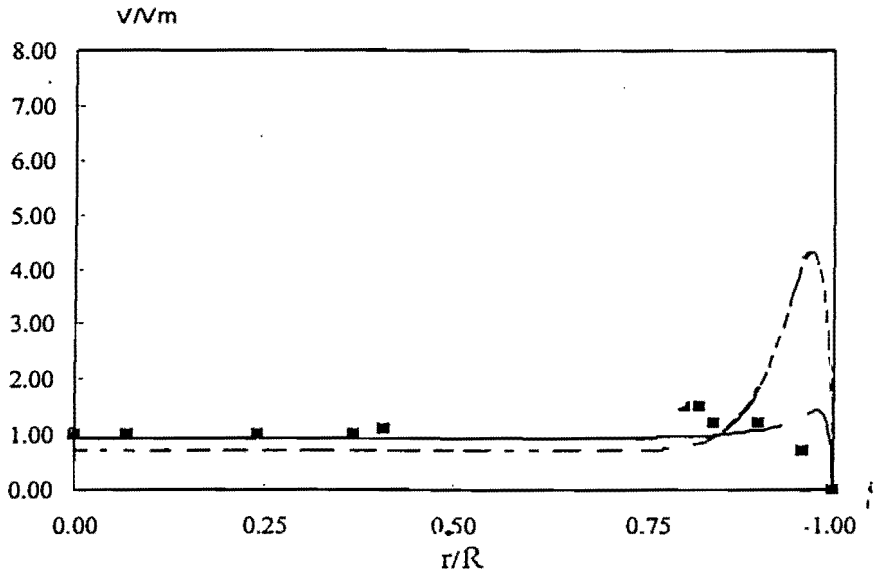

Fig.5 Comparison of velocity distributions of the present numerical results and the previously published work at Re_d=7.5, Pr=0.7 and D/d=16

- - - previous analytical solution of Vortmeyer& Schuster,1983 [14]

—— Present numerical results considering the porosity at the wall is limited to 0.44

■-previous measurements listed in Vortmeyer& Schuster,1983 [14]

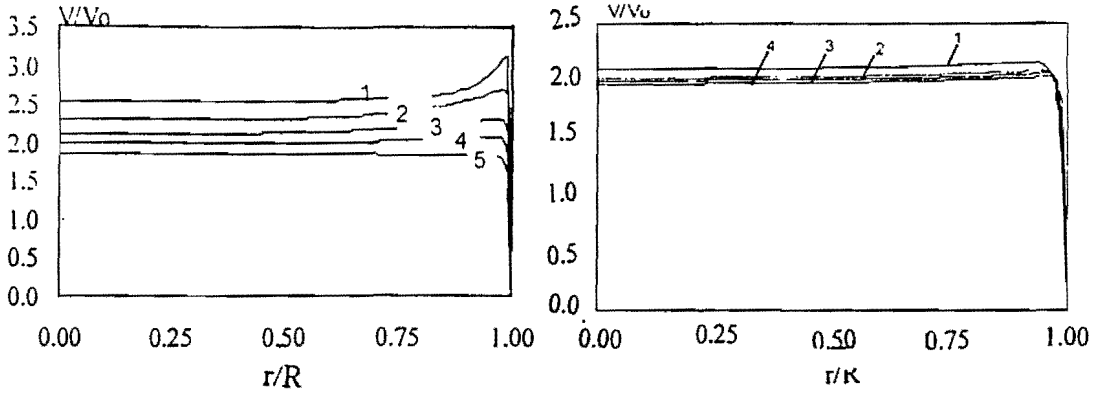

(a)

mass flow rate=0.2 kg/s

1-- D/d=16, Da=2.7x10^{-6}, γ=365.4, Red=625.2 and P*=910.6

2-- D/d=6.4, Da=2.11x10^{-5}, γ=135, Red=1563.1 and P*=248.9

3-- D/d=4, Da=6.9x10^{-5}, γ=77.1, Red=2501.2 and P*=110.2

4-- D/d=3.2, Da=1.3x10^{-4}, γ=57.1, Red=3126.3 and P*=69.2

5-- D/d=2.67, Da=2.36x10^{-4}, γ=43.1, Red=3751.5 and P*=44.52

(b)

D/d=3.2, Da=1.3x10-4and γ=57.1

1---mass flow rate=0.02 kg/s, Re_d=340.1 and P*=89

2---mass flow rate=0.045 kg/s, Re_d=725.9 and P*=77.2

3---mass flow rate=0.075 kg/s, Re_d=1190.22 and P*=73.2

4---mass flow rate=0.2 kg/s, Re_d=3126.3 and P*=69.3

Fig.6 Velocity distributions in radial direction inside the packed pipe at different particle sizes(a) and mass flow rates(6b)(Pr=5)

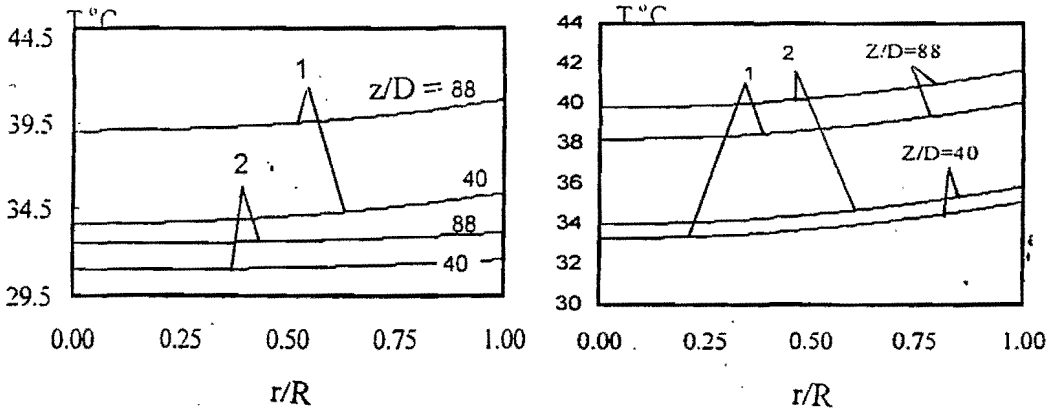

(a)

1-- Re_d=170 and P*=368.6

2--Re_d=595 and P*=272.7

(b)

1---D/d=16 γ=365.4, Da=2.77x10^{-6}, Re_d=68.2 and P*=1869.24

2---D/d=4 γ=77.1, Da=6.9x10^{-5}, Re_d=272.1 and P*=146.6

Fig.7 Effect of particle Reynods number on the radial temperature distributions due to the increase of mass flow rate (a) and the particle size(b) at Pr=5

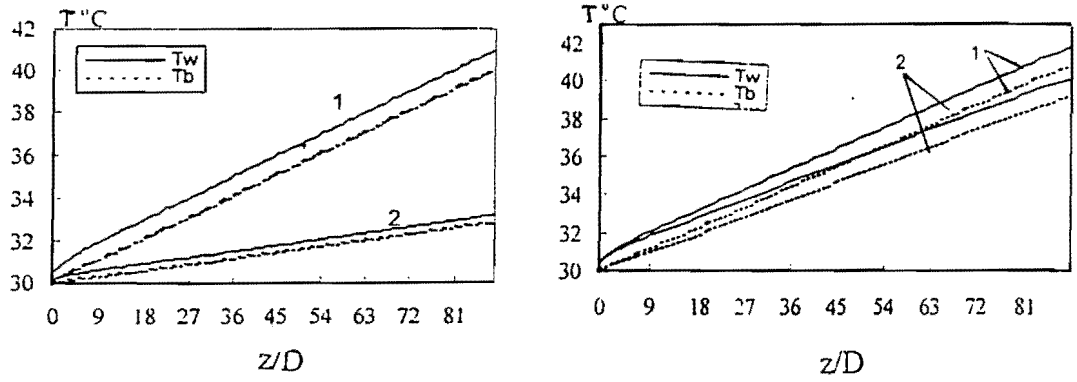

(a)

1-- Re_d=170 and P*=368.6

2--Re_d=595 and P*=272.7

(b)

1---D/d=4 γ=77.1, Da=6.9x10^{-5}, Re_d=272.1 and P*=146.6

2---D/d=16 γ=365.4, Da=2.77x10^{-6}, Re_d=68.2 and P*=1869.24

Fig.8 Effect of particle Reynods number on the axial tempe.ature distributions due to the increase of mass flow rate(a) and the particle size (b) at Pr=5

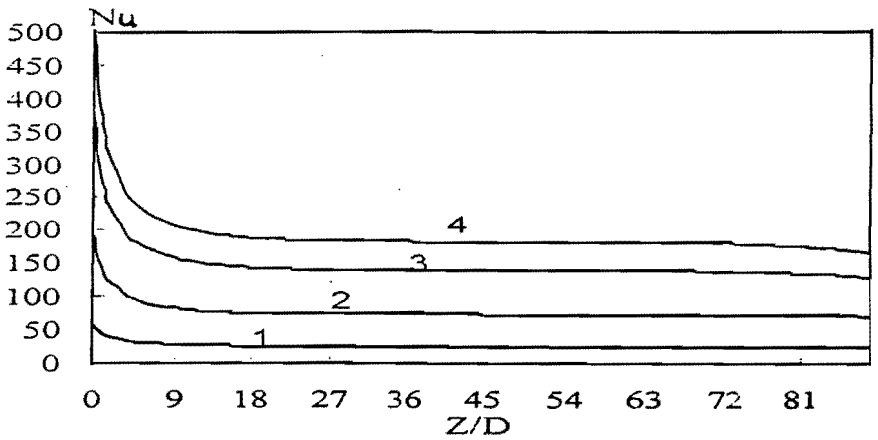

1-- Re_d=170 and P*=368.6

2--Re_d=595 and P*=272.7

1-- Re_d=1175 and P*=253.78

2--Re_d=1563 and P*=248.97

Fig.9. local Nusselt number distributions in the axial direction at pipe-surface Da=2.11x10^{-5}, γ=135.45, D/d=6.4 and Pr=5

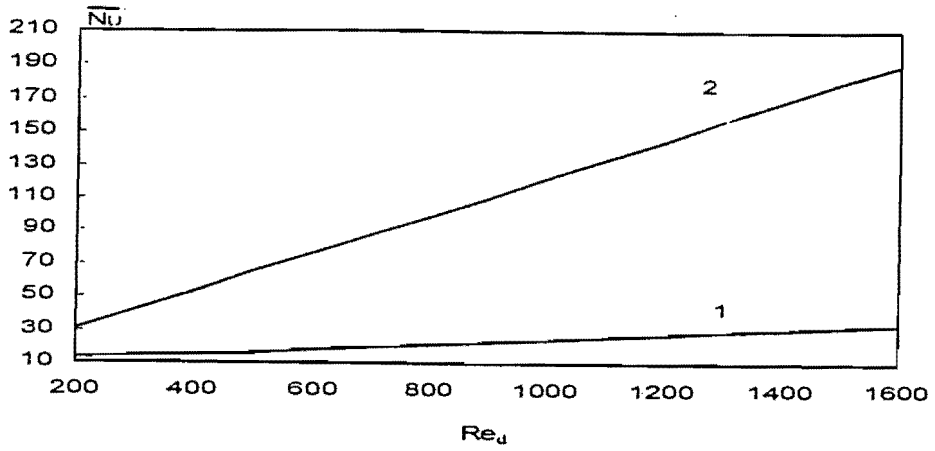

Fig.10 Variation of Nusselt number with particle Reynolds number at different Prandtl numbers for $Da=2.85\times10^{-5}$, $\gamma=117.1$ and $D/d=5.64$(1--- $Pr=0.7$ 2---$Pr=5$)

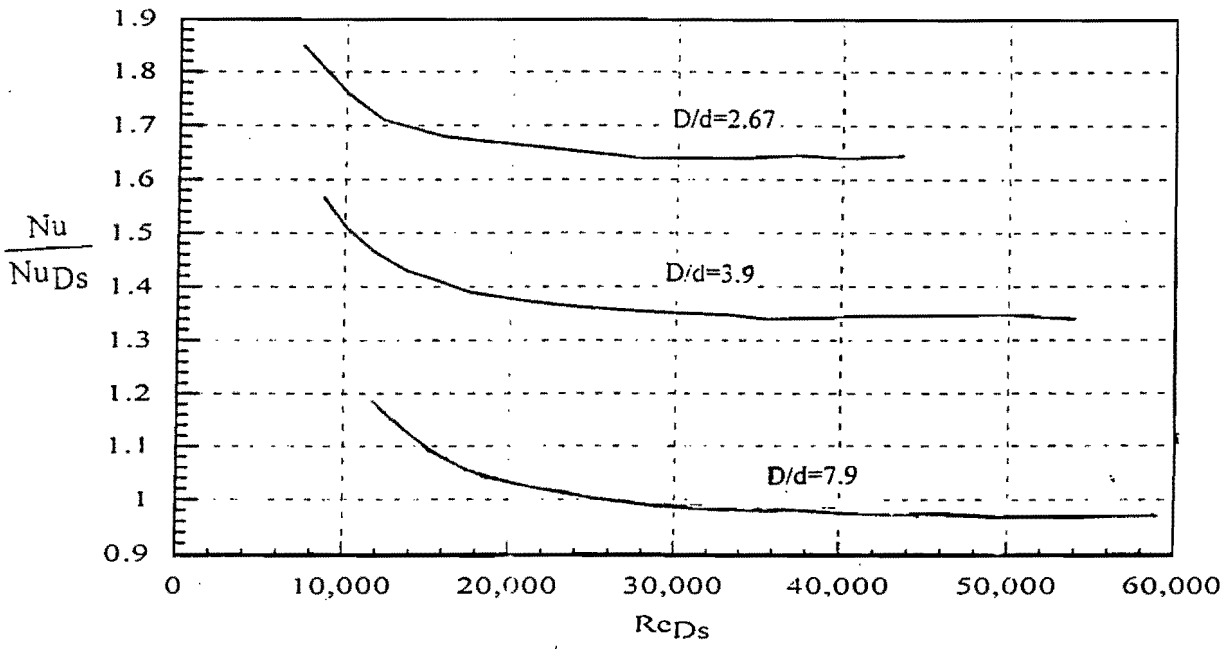

Fig.11 Heat transfer enhancement for turbulent flow with equal pumping power